AIAA JOURNAL
Vol. 39, No. 10, October 2001

Experimental Study and Simulation of Rocket Engine Freejet Noise

Jean Varnier*
ONERA, 92320 Châtillon Cedex, France

On behalf of Centre National d'Etudes Spatiales and in the framework of studies concerning the acoustic environment of Ariane 5 launcher at liftoff, ONERA has adapted a NASA jet noise model of the 1970s to the near sound field simulation. To validate this model, tests have been carried out with static rockets of various sizes. Several improvements appear to be necessary for a more accurate simulation of the near-field measurements: In particular, the characteristic length of the model must be reduced, and the fully expanded jet data must be used instead of the jet exhaust data. It is shown that the acoustic efficiency, for a given Mach number, is not dependent on the rocket size and may be estimated from a semi-empirical formula found in the literature. The model changes are checked with other jets of various characteristics. On the basis of experiments and following an approach deduced from an earlier study, the spatial characteristics of the sound field and more particularly the sound power peak location are related to the supersonic length of the flow, which appears to be the adequate reference length for a future jet noise model.

Nomenclature

c, c_x	=	speed of sound, m/s
D	=	nozzle exit diameter, m
D_x	=	jet diameter, m
$d_{x,x}$	=	distance, m
DI	=	directivity index, dB
F	=	thrust, N
f	=	frequency, Hz
$\boldsymbol{I}_x$	=	acoustic intensity vector
i	=	basis of imaginary numbers
k	=	wave number, m^{-1}
L	=	distance from the nozzle on the jet axis
L_A	=	acoustically effective jet length
L_C	=	laminar core length
L_C^*	=	experimental characteristic length
L_P, L_P^*	=	sound power peak location
L_S, L_S^*	=	jet supersonic length
M, M_x	=	Mach number
m	=	mass, kg
m_x	=	mass flow, kg/s
P_x	=	static pressure, bar
p_x, $p_{x,x}$	=	sound pressure, Pa
R	=	radius or distance, m
r	=	constant of gas, J/kg · K
Sr	=	Strouhal number
Srm	=	local Strouhal number
S_x	=	cross sectional area, m^2
s, S	=	sound source
T_x	=	static temperature, K
V, V_x	=	velocity, m/s
W_A, W_A^*	=	acoustic power, W
W_M	=	mechanical power, W
α	=	coefficient
γ, γ_x	=	ratio of gas specific heats
η, η^*	=	acoustic efficiency
θ, θ'	=	angle made with the jet axis
ρ_x	=	mass per volume unit, kg/m^3
Σ	=	nozzle area ratio (exit area / throat area)
(Σ)	=	integration surface
Φ	=	complex expression of normalized cross spectral density (NCSD)
φ	=	phase of NCSD

Indices

a	=	atmospheric (ambient) data
e	=	jet exhaust data
i	=	chamber stagnation conditions
j	=	fully expanded jet data
k	=	numerical index
t	=	nozzle throat data
x	=	small index
$*$	=	experimental data

I. Introduction

THE prediction of the noise generated by a spatial launcher is necessary for estimation of the vibroacoustic stress on the vehicle and on the payloads carried during liftoff, as well as noise pollution and its repercussions on the surroundings. Thus, for a given rocket engine, it is necessary to determine the overall sound power radiated by the jet, as well as the spectrum, the directivity, and the spatial distribution of the sound sources.

In the context of NASA's work, many experiments concerning this topic[1] have been performed by U.S. laboratories, especially from 1950 to 1970. In particular, static tests have been carried out with various types of jets and rocket engines: turbojets,[2] substitute gas jets,[3] scale models of missiles,[4] freejets,[5,6] or deflected jets[7] of small solid-fueled rockets, and single or clustered large boosters.[8] Rules of similitude have been established to extrapolate the results obtained with reduced-power jets.[4] The noise received on the ground during a launcher flight has also been studied.[9] In the latter case, the jet may be considered as a single sound source.

Simultaneously, theoretical studies based on Lighthill's theory for subsonic jets[10,11] or, using diverse assumptions, on its extension to the supersonic case, have been applied to predict the rocket or aircraft jet noise.[12–14] However, because of the complexity and of the multiplicity of the phenomena,[15] the theoretical approaches must be adapted to the experimental data in the shape of semi-empirical models.

The main difficulty is to determine a relationship between the aerodynamic characteristics of the flow and the spatial characteristics of the sound field. Answers to this problem found in the literature are diverse and sometimes contradictory.[16,17] Another difficult question concerns the estimation of the radiated overall sound power.[18]

In a synthesis report,[19] Eldred et al. summarized the results of several earlier studies and proposed a jet noise model including a

Received 25 February 2000; revision received 12 April 2001; accepted for publication 17 April 2001.

*Research Engineer, Département Simulation Numérique des Ecoulements et Aéroacoustique, BP 72.

fine representation of the acoustic sources, which seems able to simulate both the near- and far-field noise. This model has been used by ONERA for predicting the sound environment of the first Ariane launchers.[20] However, in the context of studies carried out to estimate the sound field radiated by the solid-propellant boosters of Ariane 5, tests performed with static rockets have shown that the model was not adapted for the simulation of the sound pressure measurements made in near field, essentially because of an unsuitable spatial distribution of the sound sources.

Thus, analyses show that the characteristic length used in the jet noise model must be reduced. Moreover, the fully expanded jet parameters must be used in the semi-empirical formulas instead of the jet exhaust parameters. The acoustic efficiency deduced from the experimental sound power seems to be related to the Mach number of the jet and not to the rocket size. This result is confirmed by a formula proposed by Sutherland.[21]

The validity of the model changes is checked with several jets, which are under- or overexpanded at the exhaust. In particular, aerodynamic and acoustic measurements are made with a supersonic jet tested in the MARTEL facility of the Centre National d'Etudes Spatial (CNES). The supersonic length of the jet, which appears as the adequate aerodynamic reference, may be calculated and related to the sound power peak location by simple relations deriving from empirical formulas found in a previous study.[13] These relations constitute the basis of a future jet noise model.

II. Jet Noise Prediction Method

A. General Remarks

Supersonic jet noise results from contributions of several components: Mach waves, turbulence of the mixing zone, shock cells, and screech effect. This is why a single theory cannot represent the whole intervening physical phenomena. For example, the sound power radiated from turbulence is assumed proportional to V^8 in the subsonic region[11] and to M^3 in the supersonic region.[17] The broadband shock noise,[22] which concerns jets whose static pressure at the exhaust is not equal to the ambient pressure, seems to be proportional to M^4, or more precisely to $(M_j^2 - M_e^2)^2$. Screech mechanism[23] and heat effects[24] have other characteristics. However, in the case of highly supersonic and very hot jets, the noise due to the supersonic convection of the eddies (Mach waves and supersonic turbulent shear noise) becomes dominant, and the sound power stays more or less proportional to M^3.

Finally, the models that are able to reproduce and to predict (at least in far field) the sound field of supersonic jets, are essentially of an empirical type. For instance, the theoretical considerations that are developed by Potter and Crocker's freejet noise model[12] disappear almost completely in a similar model presented by Eldred et al.[19] and are replaced by purely experimental data. Remember that these data sometimes come from experiments or extrapolations obtained with subsonic or cold supersonic jets,[16] which can give questionable results in the case of rocket engine jets, as suggested in a recent paper.[25]

The same remark applies to Lighthill's jet noise theory[10,11] extended to the supersonic case. As a consequence, it was assumed that the turbulent mixing noise remains the dominant noise source.[26] Also we can note that the laminar core, which often is taken as an aerodynamic reference, is difficult to define in the presence of shock cells. In fact, one rarely finds in the acoustics papers considerations concerning the aerodynamic characteristics of a jet, such as the aerodynamic measurements of Ref. 27.

B. Freejet Noise Model

Here we describe a jet noise model recommended by Eldred et al.[19] for predicting the rocket engine noise. This model uses as characteristic length the core length of the flow, given by an empirical formula first established by Lighthill[10,11] with subsonic cold jets:

$$L_C = 3.45 D_e (1 + 0.38 M_e)^2 \tag{1}$$

in which the jet exhaust diameter D_e is taken equal to the nozzle exit diameter D. As pointed out in Ref. 1, Cole et al.[6] propose another expression for the rocket engine jets, which gives results contradictory to this formula for large Mach numbers. Note that Eldred et al.[19]

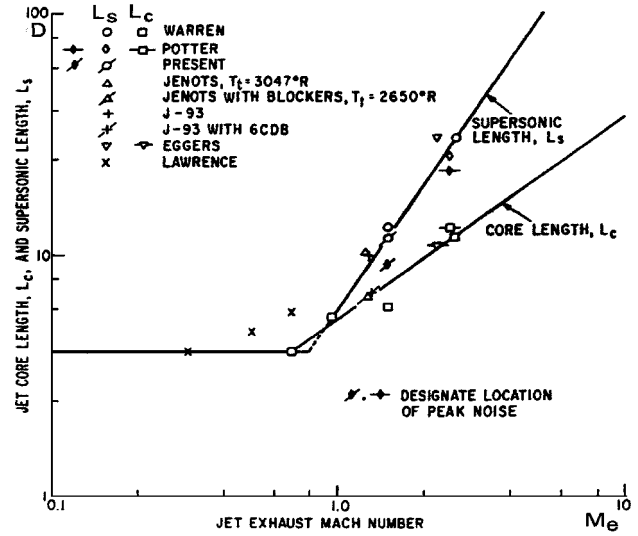

Fig. 1 Laminar core length and supersonic length, as a function of the exhaust Mach number, from Ref. 13; Potter's data are those of Ref. 16.

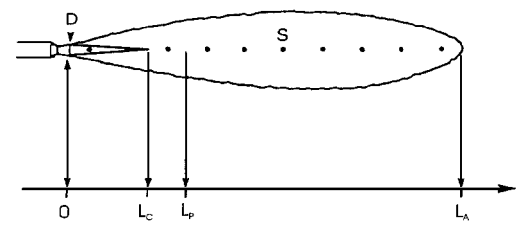

Fig. 2 Acoustic model of freejet: discrete sound sources S and conventional lengths. (The supersonic length L_S is not specified or used in Ref. 19.)

justify the use of Eq. (1) in the case of rocket jets by dividing by two their supersonic lengths given in Ref. 27. Thus, the supersonic core (defined by a nonturbulent flow) here seems to be around 50% smaller than the supersonic region of the flow.

In the literature, the jet core is sometimes called the laminar core[1,16] and sometimes the supersonic core.[13,19] In fact, a careful reading shows possible confusion between laminar core, supersonic core, and supersonic region. In Ref. 27, the supersonic core is likened to the supersonic region defined upstream from the sonic point. Also, in Ref. 1, the supersonic core length given by Eq. (1) clearly designates the length of the supersonic region and not the laminar core length. On the contrary, in Ref. 13, supersonic core length and supersonic length are calculated by two distinct formulas:

$$L_C = D_e\left(5.22 M_e^{0.9} + 0.22\right) \tag{2}$$

$$L_S = D_e\left(5 M_e^{1.8} + 0.8\right) \tag{3}$$

The authors write M_e^2 in second formula, but take $M_e^{1.8}$ in the applications. It is interesting to note that the ratio L_S/L_C increases with the exhaust Mach number M_e, but is close to 1 for $M_e = 1$ (Fig. 1).

To avoid possible ambiguities, we now only use the expressions laminar core length for L_C and supersonic length for L_S.

In fact, the length of the jet supersonic region does not appear explicitly in the Eldred et al. jet noise model,[19] the main conventions of which are presented in Fig. 2. The overall sound power is distributed along the jet axis, using discrete sound sources S and following the experimental curve of Fig. 3 (the original references are indicated in the captions of the figures). We can see that the sound power peak is located at the distance from the nozzle:

$$L_P \approx 1.5 L_C \tag{4}$$

Figure 3 also shows that the acoustically effective length of the jet (which here represents at least 98% of the overall sound power) has an approximate value of

$$L_A \approx 5 L_C \tag{5}$$

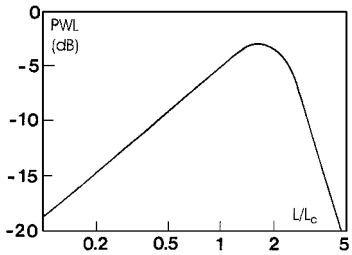

Fig. 3 Distribution of the sound power along the jet axis, for standard chemical rockets (0 dB is the reduced OAPWL of the jet) (from Refs. 12, 16, and 19).

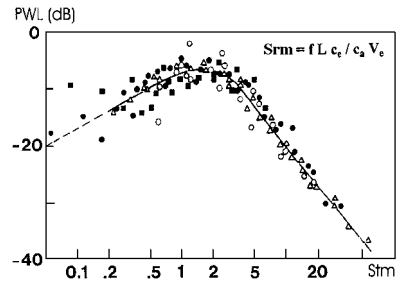

Fig. 4 Dimensionless noise spectrum, for standard chemical rockets (0 dB is the reduced sound power level of the sound source located at *L*) (from Refs. 3, 5, 16, and 19).

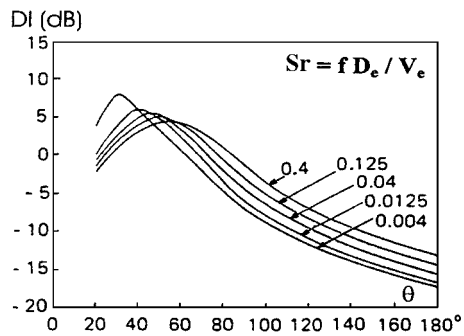

Fig. 5 Jet noise directivity in far field, for standard chemical rockets (0 dB is the directivity index of a monopole, 180 deg is the upstream direction) (from Refs. 3, 6, 7, and 19).

The sound power spectral density of a discrete source S located at L on the jet axis is given by the experimental curve of Fig. 4, related to a local Strouhal number:

$$Srm = fLc_e/c_aV_e \tag{6}$$

The value of the spectrum peak frequency of the source that occurs for $Srm \approx 2$ appears to be inversely proportional to its distance from the nozzle. Thus, the highest frequencies are radiated near the nozzle and the lowest frequencies far from the nozzle. Also, we can see that the peak frequency of a large rocket will be lower than the one of a small rocket for given exhaust velocity and temperature, the sound power peak on the jet axis being farther from the nozzle.

At last, the mean directivity of the sound sources is given by the directivity curves of Fig. 5, as a function of the Strouhal number (dimensionless frequency):

$$Sr = fD_e/V_e \tag{7}$$

Theses curves are discussed in Ref. 21, in which another model of directivity is proposed.

The sources of the model are assumed uncorrelated, and the sound pressure at a given point of space results from the contribution of each source, following a $1/R$ decrease law.

As written in the preceding equations, the physical data used are generally the jet exhaust data. However, Eldred et al.[19] indicate that index e corresponds to "the nozzle exit data (fully expanded)." However, D_e still remains equal to the nozzle exit diameter, and not to the theoretical diameter of the fully expanded jet.

C. Acoustic Power

The overall sound power of the jet is a basic input data of a jet noise model, which justifies a specific section. In Refs. 5, 12, and 18, many ways for estimating the overall sound power are indicated. The acoustic efficiency η, defined by

$$\eta = W_A/W_M \tag{8}$$

is usually taken equal to 0.5% in the case of the rocket jets. However, in Ref. 18 it is indicated that its value increases with the mechanical power of the rocket.

More recently, Sutherland,[21] for an estimation of the acoustic efficiency based on aerodynamic characteristics of the flow, has proposed the relationship:

$$\eta = K(\gamma_j/\gamma_a)(c_t/c_a)^3(c_t/V_e)^2 \tag{9}$$

where K is an experimental factor equal to 0.0012. A statistical analysis takes into account data coming from jets, rockets, and boosters representing a large range of mechanical power ($10^4 W < W_M < 10^{11} W$), and gives for η a mean value of 0.53% with an uncertainty of $\pm 0.24\%$, which does not seem to be correlated with the jet mechanical power.

In the same paper,[21] the mechanical power is given equal to $0.5m_tV_e^2$, which represents the kinetic energy of the gases at the exhaust, but does not include the potential energy due to the difference between the jet static pressure at the nozzle exit and the atmospheric pressure. Therefore, an expression independent of the shape of the nozzle is preferable:

$$W_M = 0.5m_tV_j^2 \tag{10}$$

Also, the thrust may be easily calculated by the formula

$$F = m_tV_j \tag{11}$$

It is interesting to know the mechanical power of a rocket engine jet and to be able to estimate directly its acoustic efficiency because the experimental estimation of the sound power W_A constitutes a difficult problem. However, under some conditions and hypotheses, the sound power may be estimated from sound pressure measurements made in far field.[5,8,9]

III. Acoustic Simulation of Rocket Firings

A. Static Tests of Solid-Fueled Rockets

It is admitted that the sound power radiated by a highly supersonic jet is more or less proportional to V^3 and so to its mechanical power. To verify this rule and to validate the jet noise model at reduced scale, ONERA has chosen to test several small or medium sized rockets with similar characteristics[28] in the Fauga–Mauzac Test Center.

The jet noise model described earlier, which includes a fine representation of the sound sources, seems able to simulate the acoustic near field which is of interest for a launcher at liftoff. Here we define the near field as the region where the spatial distribution of the sound sources must be taken into account for an accurate simulation of the sound field. Of course, it is clear that the correlation effects in the vicinity of the jet due to the shock noise will be ignored.

Thus, the measurement device has been deployed relatively close to the rockets. The rocket is horizontally fired, about 1.05 m above the ground, which is quasi perfectly reflective (concrete surface). The microphones are in the horizontal nozzle plane, at distances from the nozzle in the range $5D$–$40D$ (D is the nozzle exit diameter of the considered rocket). Some of these are distributed along an arc of a circle of radius $20D$, another part forms a linear array parallel to the jet axis. The rocket is put ahead of a cavity lined by a wall, which is partly treated against noise (thin absorbent moss layer on the doors, see the serrated lines in Fig 6).

To minimize the acoustic reflections effects, the microphones used are 1:4 in. Brüel&Kjaer pressure microphones, which are relatively directive, turned toward the jet. Also, a thin absorbent moss layer is placed on the ground only below the microphones on the left side of the jet axis (an error which has introduced many difficulties in the analysis).

Table 1 gives the main characteristics of some tested rockets. The aerodynamic characteristics are similar for the jets of all of the rockets and respect the similarity laws[4,20] compared with the boosters of Ariane 5. The Mach number is related to the local sound speed. The

Table 1 Main characteristics of rockets tested by ONERA

Rocket number	D, cm	F, kN	W_M, MW	m_t, kg/s	P_e, bar	M_e
5	3.56	0.7	0.85	0.29	0.7	3.3
2	7.11	3.8	4.5	1.59	0.7	3.3
1	14.25	14.3	17.7	5.86	0.7	3.3
0	26.72	58.4	72.6	23.6	0.7	3.3

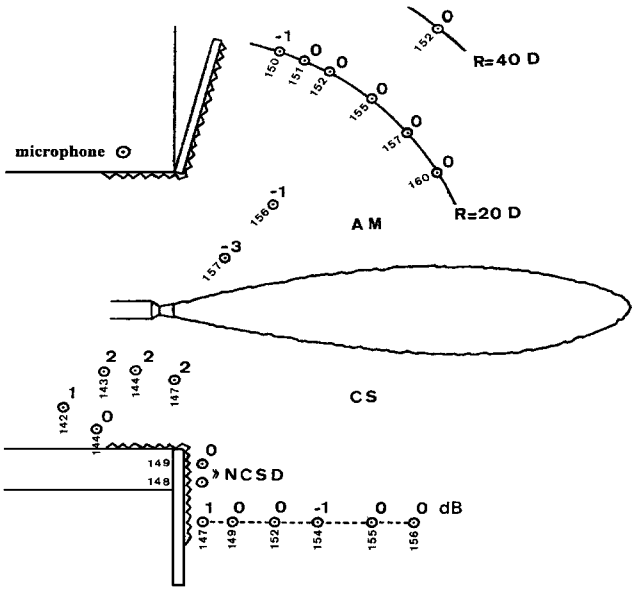

Fig. 6 Rocket 0: recorded OASPL and measurement–computation differences (dB), where AM = absorbent moss and CS = concrete surface; distance $R = 40D$ is shortened.

rockets are loaded with a composite propellant (NH_4ClO_4–$(C_4H_6)_n$–Al), which allows representative exhaust velocity ($V_e \approx 2500$ m/s) and exit Mach number during a burning time of about 1.2 s. The jets are overexpanded at the nozzle exit. The area ratio Σ of the convergent–divergent nozzle is equal to 10.

B. Acoustic Analyses

A classical method for calculating the radiated sound power is to consider the sound pressures measured on the microphone arc and the integration surface generated by the rotation of this arc around the jet axis. The modulus of the sound intensity vector, assumed normal to the surface, is deduced from the rms sound pressure. Note that this method, which is used but not precisely described in Ref. 5, assumes the revolution symmetry of the acoustic field and takes as negligible the effects of sound reflections off the ground. Moreover, the integration surface must include the sound source region over a broad range.

It is not the case here, and a radius of $20D$ has proved to be too small for an accurate sound power calculation. When the length of the luminous jet plume is considered, estimated from pictures of the firings to be at least $30D$, it was clear that the sound source region was extended beyond the measurement arc. This was confirmed by the very strong sound pressures measured downstream near the jet axis (160 dB). However, a first estimation of the radiated sound power[28] has been made using the method described earlier, which shows an acoustic efficiency increasing with the rocket size from 0.4 to 0.6%.

In fact, a more precise analysis based on numerical simulations has suggested that this variation was related to the reflected sound field over the moss, which is not perfectly absorbent. Indeed, it was probable that great similarities exist between the sound pressure levels measured with rockets of different sizes for given dimensionless frequencies because of the adaptation of the measurement device, the scale of which was related to the nozzle diameter. Unfortunately, however, the unmodified distance of nozzle-to-ground does not remain in the same scale, being close to $4D$ with the largest rocket and $30D$ with the smallest. Thus, the ratio of the reflected sound pressure and the direct sound pressure in the plane containing the microphones is not constant: Analyses of the sound pressure levels recorded over the moss and over the reflective ground have shown appreciable disparities according to the rocket size. Finally, it appeared that it was not possible to ignore the reflection phenomena and to calculate the sound power in a reliable manner using a classical integration method.

Therefore, another approach based on the numerical simulation of the recorded sound pressure levels (SPLs) has been adopted. In this method, the overall sound power is introduced as free input data into the computer code. The sound field computation takes into account the acoustic reflections off the ground, considering an image jet symmetrical to the actual jet. The assumed experimental overall sound power is the sound power value introduced to reproduce at best the SPL measurements over the reflective ground, by minimization of the mean squares of the measurement–computation differences.

An associated problem is to calculate the real efficiency of the absorbent moss, by assuming the lateral symmetry of the radiated sound field. From an accurate simulation of the sound levels over the reflective ground, the corrections due to the moss presence on the other side can be determined from statistical differences between computed and recorded levels for the concerned microphones. These corrections, which stay in the range from 0 to -2 dB according to the frequency and the scale of the test, concern the sound levels due to the image sources. Of course, the microphone arc over the moss is rather a witness for the directivity.

In contrast, the cavity and wall effects have been assumed as negligible: Indeed, a calculation based on the directivity curves of Fig. 5 shows that 90% of the jet overall sound power is radiated in the downstream direction. Thus, the possible error in the sound level estimation due to the rear echo cannot exceed $+0.5$ dB.

Figure 6 shows the recorded overall SPL (OASPL) for rocket 0 and the differences in computation–measurement after adjustment of the sound power. The greatest differences appear as expected in the region close to the nozzle, where the shock noise may be dominant. Note that a classical accuracy[19,21] for this type of model is ± 2 dB in overall level, which is verified here in near field. In octave level, the uncertainty is ± 4 dB, the sound power spectrum of the model being more peaked than the actual.

Table 2 indicates the overall sound power level (OAPWL) introduced in the computer code for an accurate simulation of the recorded OASPL, and the corresponding experimental sound power W_A^*. The experimental acoustic efficiency η^* is obtained from the ratio W_A^*/W_M. The found values are larger than those obtained with the previous method, which neglects the sound sources beyond the microphone array.

Note that this simulation method has been applied after preliminary modifications of the jet noise model, which are described in the next section. These changes introduce additional uncertainties, which are quite difficult to estimate. Therefore, it is necessary to compare the found values η^* of the acoustic efficiency with the statistical values η given by the semi-empirical Eq. (9). We can see that the agreement is generally good, which seems to constitute a first validation of the modified model and of the sound power evaluation method. Moreover, the unchanging values of η^* or η show clearly that the acoustic efficiency is related to the jet Mach number[13] rather than to the rocket size.[18]

The anomaly for rocket 5 ($\eta^* \approx 1\%$) is most probably due to the microphone grid effects: As shown in Fig. 7, recorded in the presence of a supersonic jet noise, the grid introduces an SPL enhancement

Table 2 Experimental and statistical acoustic characteristics of tested rockets

Rocket number	D, cm	W_M, MW	OAPWL*, dB	W_A^*, kW	η^*, %	η, %
5	3.56	0.85	159	8	0.9	0.6
2	7.11	4.50	165	32	0.7	0.5
1	14.25	17.7	171	126	0.7	0.6
0	26.72	72.6	177	500	0.7	0.6

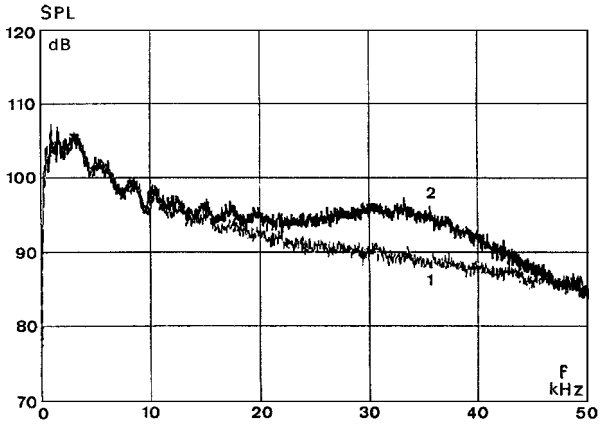

Fig. 7 Jet noise sound pressure spectrum, recorded with 1:4 in. Bruël and Kjaer pressure microphones: curve 1, without protection grid and curve 2, with protection grid.

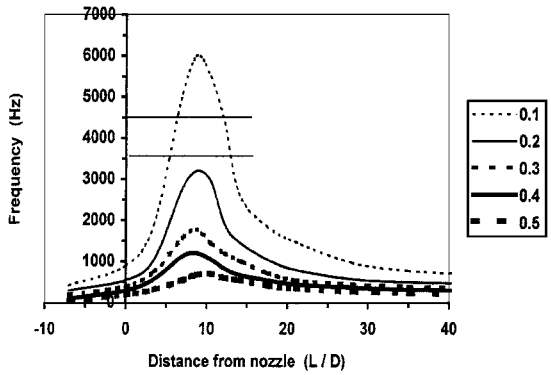

Fig. 8 Firing of rocket 2 ($D = 7.11$ cm): square coherence $\|\Phi\|^2$ obtained using the focused array method for sound sources located on the jet axis. The cutoff frequencies of the octave, the sound power level of which is dominant, are indicated by horizontal lines.

above 10 kHz, in a frequency range more particularly concerned by the spectrum of this small rocket. Thus, its actual acoustic efficiency is probably similar to the other ones. Note that the frequency peak in octave band varies from 1 kHz for the largest rocket to 8 kHz for the smallest, which is well calculated by the model.

Other acoustic analyses have been made: 1) spatial correlation between two neighboring points of the sound field, in the form of recorded and computed normalized cross spectral density (NCSD) and 2) sound sources localization, thanks to the linear array of 19 microphones drawn partly on Fig. 6 (dashed line), using a conventional focused array processing.[29,30]

Both methods are based on the analysis of the signal correlation between the microphones, which gives the phase differences and, therefore, the main direction of sound propagation. The NCSD is very sensitive to the spatial distribution and to the correlation of the sound sources, and constitutes a good witness for the exactness of the physical model (see Appendix A). The focused array method allows the localization of the apparent sources on a known line, here the jet axis. However, the expanded character and the strong directivity of the sound sources of the jet are not favorable to a precise localization of the sound peak: For all of the rockets, the sound sources corresponding to the frequencies of the peak in the octave band level were found to be between 5 and 15 exit diameter D from the nozzle (Fig. 8). We can assume that this interval includes the actual sound power peak location L_P^*.

IV. Modified Jet Noise Model

A. Basis Hypotheses and Experimental Adjustments

For the tested rockets, Eqs. (1) and (4) of the jet noise model described in Sec. II.B give the sound power peak location $L_P \approx 26D$, outside the measurement device. With such a sound source distribution, the overall sound power that is necessary for approaching the recorded SPL values appears totally unrealistic ($\eta \approx 3$–4%). In fact, for a more suitable simulation of the near sound field, three hypotheses may be made.

1) The characteristic length must be reduced: from comparison between the experimental location of the sound power peak L_P^* indicated in Sec. III.B and the calculation result indicated earlier, factor 3.45 of Eq. (1) is divided by two.

2) Equation (1) and the others are written using the fully expanded jet data instead of the jet exhaust data, assuming that the nozzle shape has a minor influence on the jet characteristics.

3) The far-field directivity given by the curves of Fig. 5 is slightly modified to take into account the spatial distribution of the sound sources (see Appendix B).

Thus, Eq. (1) giving the characteristic length of the model is replaced by the following formula:

$$L_C^* = 1.75 D_j (1 + 0.38 M_j)^2 \tag{12}$$

in which D_j is the theoretical diameter of the fully expanded jet, which may be calculated using the relationship deduced from the state equation of ideal gases (see Appendix C)

$$D_j = (2/M_j)(m_t V_j / \pi P_a \gamma_j)^{\frac{1}{2}} \tag{13}$$

In this formula, the mass flow m_t is assumed constant and equal to its value at the nozzle throat. For the rockets tested by ONERA, we have $M_j \approx 3.1$ and $D_j \approx 0.9 D_e$. Note that D_j also represents the nozzle exit diameter for a jet perfectly expanded at the exhaust.

For convenience, the lengths calculated in the following discussion are related to the nozzle exit diameter D. For the tested rocket jets, the mean sound power peak location L_P^* given by Eqs. (12) and (4) is close to $11D$, which is included in the range $5D$–$15D$ found from focused array processing.[29]

B. Test of the Model Changes

Our purpose in Sec. IV.A was to adjust a tool and to define general rules for its parameter, to be able to predict the sound field radiated by other rocket engines.

However, the tested rocket jets are very similar, and first it appears necessary to confirm the model changes by considering several jets of various characteristics. The main questions concern the characteristic length, much shortened in the modified model, and the choice of the fully expanded jet parameters.

To make a comparative study, we consider in Table 3 several rocket engines of various types and in Table 4 the main characteristics of their jets.

Rita II is a stratospheric solid-fueled booster of a ballistic missile, which has been fired in CAEPE Center in similar conditions to those of the Fauga-Mauzac Test Center (horizontal static firing), but with a more complete measurement device: In particular, two

Table 3 Chamber stagnation conditions and nozzle characteristics of several rocket engines

Parameter	Rita II	Rocket 0	Rocket F	Jet IV	Unit
P_i	57	64	55	30	bar
T_i	3250	3300	2850	1040	K
m_t	101	23.6	4.41	1.71	kg/s
D	84	26.72	7.33	6	cm
Σ	21	10	3.7	6	——

Table 4 Jet exhaust data and fully expanded jet data of several rocket engines

Parameter	Rita II	Rocket 0	Rocket F	Jet IV	Unit
D_e	84	26.7	7.33	6	cm
M_e	3.8	3.3	2.6	3.3	——
V_e	2650	2550	2000	1270	m/s
P_e	0.3	0.7	2.5	0.5	bar
D_j	52.0	24.5	10.2	4.8	cm
M_j	3.1	3.2	3.1	2.8	——
V_j	2410	2480	2200	1200	m/s
P_j	1.0	1.0	1.0	1.0	bar

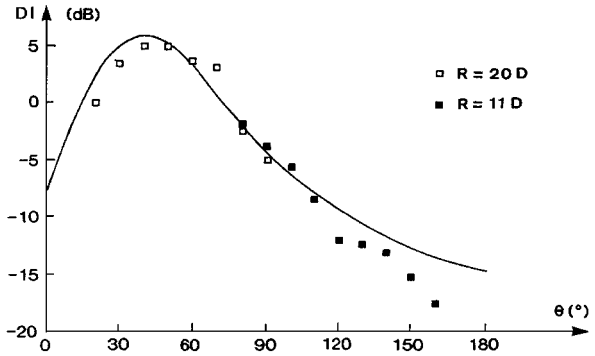

Fig. 9 Firing of missile Rita 2 ($D = 84$ cm): directivity deduced from SPL measurements on two arcs of microphones (squares), and directivity deduced from SPL computations based on the modified jet noise model (curve).

microphone arcs of radius $20D$ and $11D$ are installed, respectively, downstream and upstream from the nozzle. The jet is very overexpanded at the ground level (possible existence of a shock disk) and the sound emission appears to be unstable. However, a satisfactory simulation of the averaged SPL may be obtained (see the corresponding directivities in Fig. 9). According to this simulation, the jet characteristic length L_C^* seems to be 20% shorter than given by Eq. (12). The found acoustic efficiency is close to 0.6–0.7%.

Rocket 0 is the largest rocket tested in Fauga-Mauzac Test Center (see Sec. III.A).

Rocket F is a rocket studied in Ref. 5, which uses a nitroglycerin–nitrocellulose propellant. Some data have been calculated using an ideal gas fluid dynamics model. The firing conditions are close to those of the previous rocket. Near- and far-field measurements have been made with this rocket, which jet is underexpanded at the exhaust. The far-field measurement arc has a radius of around $200D$. Deduced from the SPL contours recorded in the near field, the location of the sound power peak is estimated by the authors at $20D$ or more from the nozzle. The experimental acoustic efficiency is given equal to 0.65%.

Jet IV is produced in the MARTEL facility of CNES, which includes a nozzle vertically suspended over a reflective ground and supplied with an air–hydrogen mixture. The distance ground-to-nozzle has a value of $50D$, which is assumed sufficient for freejet conditions, except the acoustic reflections. However, the calculations taking the ground into account show that these reflections have a minor influence on the resultant sound field. The near-field SPL contours have been established thanks to a microphone array of step $4D \times 4D$ shifted along the jet axis (Fig. 10 on the left). Acoustic efficiency of 0.6% is deduced from an integration of the sound power on a hemisphere of $70D$ radius centered on the ground. The sound field is simulated based on this result and Eq. (12) (Fig. 10 on the right).

By comparison of the real and the computed directivity patterns, it can be seen that the actual sound power peak on the jet axis L_P^* seems to be a bit farther from the nozzle than the one given by the model (respectively, about $12D$ and $10D$). However, the agreement between real data and model data appears very satisfactory.

Figure 11 shows for these rocket engine jets a comparison between the estimated real locations L_P^* of the sound power peak, the locations L_P^e resulting from Eqs. (1) and (4), and the locations L_P^j resulting from Eqs. (12) and (4): The use of the fully expanded jet parameters instead of the jet exhaust parameters is here clearly validated. Remember that the nozzle exit diameter D is used by convenience, but that the true reference is the fully expanded jet theoretical diameter. For instance, we always have

$$12D_j \le L_P^j \le 13D_j, \qquad 10D_j \le L_P^* \le 15D_j \qquad (14)$$

Therefore, the uncertainty concerning the empirical factor 1.75 of Eq. (12) can be temporarily estimated at ±20%.

Another question concerns the estimation of the acoustic efficiency from the general characteristics of a given rocket engine. One finds in the literature that acoustic efficiency depends on the

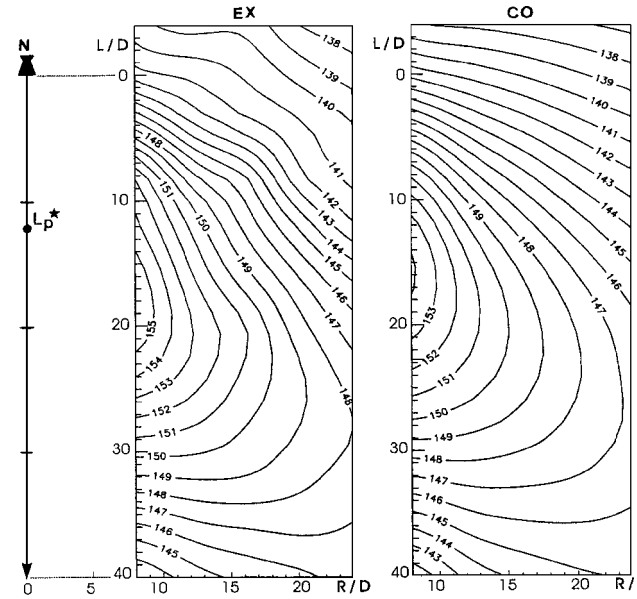

Fig. 10 Jet IV of MARTEL facility: experimental (EX) and computed (CO) OASPL contour lines. SPL are given in dB, referred to 2×10^{-5} Pa. N is the nozzle and L_p^* the apparent sound power peak deduced by comparing the model data and the real sound field.

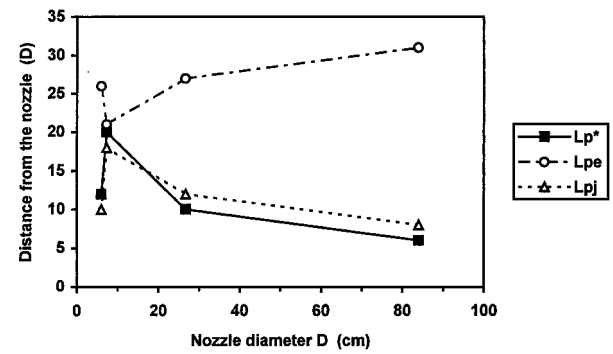

Fig. 11 Sound power peak location on the jet axis, for four different rocket jets: L_p^* is apparent location, *Lpe* location deduced from the original model, using the jet exhaust characteristics, and *Lpj* location deduced from the modified model, using the fully expanded jet characteristics.

rocket size,[18] the exhaust Mach number,[13] the nozzle shape, and the static pressure at the exhaust.[5] Equation (9) takes into account a set of thermodynamic data via the throat characteristic velocity c_t, the nozzle shape via the square exhaust velocity V_e^2, and other aerodynamic factors. The values of η calculated for strongly over- and underexpanded jets using this formula are reasonable and in the predicted range of uncertainty: 0.45% for Rita II and 0.6% for rocket F. Only the value 0.2% calculated for the slowest jet (jet IV, $W_M \approx 1.2$ MW) looks too small. Note that 0.6% is a good approximation of the experimental mean value of η for all considered rocket engines.

C. Aerodynamic Viewpoint and Generalization

Equation (12) giving the experimental characteristic length L_C^*, which has probably no aerodynamic meaning, seems to constitute a weak point in the proposed model. Now we search to relate more precisely the jet acoustic data to its aerodynamic characteristics. In fact, only two of these characteristics seem physically objective and clearly determined, namely, the sound power peak position on the jet axis L_P and the flow supersonic length L_S, knowing that the laminar core length L_C is not easy to define in the presence of shock cells, which correspond to local variations of pressure, temperature, and velocity.

In the subsonic case, it is admitted that the sound power peak location corresponds more or less to the laminar core tip. In the

sonic case, the sonic region obviously is identical to the laminar core, and then we have, for $M_j = 1$,

$$L_S \approx L_C \approx L_P \tag{15}$$

In the supersonic case, a classical hypothesis assumes the sound power peak located just before the supersonic tip[16] or more generally in the supersonic–subsonic transition region of the flow.[1,5,26] In fact, this hypothesis seems to be a necessary consequence of the extension of the subsonic jet noise theory to the supersonic case, which assumes that the most important noise source remains the turbulent mixing noise (in Ref. 5, it is clear that the supersonic length of the jet of rocket F is estimated at around $20D$ from sound field considerations).

Another theory[17] considers the supersonic turbulent convection and the Mach waves as the major noise source, which suggests a sound power peak closer to the nozzle. Because Ref. 19 indicates that the sound power peak is located beyond the jet core, it seems legitimate to write, for $M_j > 1$,

$$L_S > L_P > L_C \tag{16}$$

The ratio of Eqs. (3) and (2) from Ref. 13 suggests the approached relation, in agreement with identities (15) and (16):

$$L_S/L_C \approx M_e^{0.9} \tag{17}$$

Therefore, a similar relationship between L_S and L_P can be sought under the form

$$L_S/L_P \approx M_j^{\alpha} \tag{18}$$

where α is a parameter that remains to be determined.

Intrusive measurements using pressure and temperature coupled probes were made by ONERA with jet IV of Table 3. These measurements have allowed, from recorded stagnation pressures and temperatures, the establishment of the Mach number profiles of the jet (Fig. 12).

The Mach number M here is defined by the ratio of the local data V/c. The Mach 1 contour line, which determines the supersonic length L_S^*, runs through the jet axis at $26D$ from the nozzle. The same contour line of the Mach number referred to the ambient sound velocity, $M_a = V/c_a$, often used in jet acoustics,[1] runs through the jet axis at $28.5D$ from the nozzle. In fact, the uncertainty of the process is not easy to estimate, knowing that calculations have to take into account the shock upstream from the probes, etc. However, notice that an experimental curve of Ref. 27 gives $L_S \approx 28D$ for a Mach number of 2.8.

Also, we note that the jet acoustically effective length L_A, which may be estimated from model data at $40D$ at the most, does not very much exceed the supersonic region. An identical conclusion is suggested by Potter and Jones[16] for a cold helium jet of Mach number 2.5.

Note that Eq. (3), written with the fully expanded jet parameters

$$L_S = D_j\left(5M_j^{1.8} + 0.8\right) \tag{19}$$

here gives a correct estimation of the supersonic length ($33D_j$ or $26D$). According to Eq. (19), the underexpanded jet of rocket F has a supersonic length of $39D_j$ or $54D$. This estimation and the sound power peak location ($20D$ or more) seem to be consistent with the preceding results.

When the probable values of L_S and L_P for jet IV and rocket F were introduced in Eq. (18) with the Mach numbers of these jets, we found $\alpha \approx 0.8$ or 0.9. Of course, this estimation needs to be confirmed from other experiments and simulations.

Thus, Eqs. (19) and (18), which give the jet supersonic length and the sound power peak location according to the Mach number, are the basis of the future jet noise prediction method, knowing that the use of the fully expanded jet data constitutes the key to the problem.

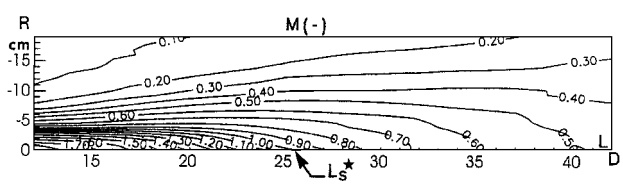

Fig. 12 Jet IV of MARTEL facility, from $L = 12D$ to $42D$ (radius R is multiplied by two). Experimental contour lines of Mach number refer to the local sound speed; L_s^* designates the jet supersonic length.

V. Conclusions

A freejet noise model from NASA's studies has been used for simulating the near-field noise of several static rockets, to establish extrapolation rules for the large boosters of a launcher. To obtain an accurate location of the sound power peak on the jet axis, the characteristic length used by the model must be modified. Instead of the jet exhaust parameters, the use of the fully expanded jet parameters in the semi-empirical formulas appears to be necessary, except to estimate the acoustic efficiency.

These changes have been successfully checked by considering other tests of rocket engines of various characteristics. In particular, aerodynamic and acoustic measurements made with an experimental air–hydrogen jet did allow the establishment of Mach number and sound pressure level contour lines. Thus, the sound field characteristics may be related to the jet aerodynamics. The simulation of the near field is in good agreement with the experiment.

In the current state of the study, we can consider as valid the following observations concerning the noise of a very hot and highly supersonic jet:

1) The adequate aerodynamic length for predicting the spatial characteristics of the radiated sound field is the jet supersonic length.

2) The location of the sound power peak, closer to the nozzle than generally admitted, may be related to the supersonic length via the Mach number of the fully expanded jet.

3) The length of the acoustically effective region of the flow does not substantially exceed its supersonic length.

4) For a given nozzle shape, the acoustic efficiency does not seem to change with the rocket size, if the Mach number of the fully expanded jet remains constant.

5) The acoustic efficiency may be estimated with a satisfying accuracy from a semi-empirical formula found in the literature.

The main difficulty of the method concerns the calculation of the jet supersonic length. An existing relationship written using the fully expanded jet data seems to give satisfactory results.

Thus, the sound field radiated by the freejet of a rocket engine now may be correctly predicted. However, the model must be adapted to the complex configuration of a launcher at liftoff. A subsequent paper will discuss the case of a supersonic jet impinging on a large plate.

Appendix A: NCSD

The computer code gives the SPL in one point, or the sound field spatial correlation between two neighboring points, in the form of NCSD. The sound sources of the jet are presumed to be uncorrelated. Therefore, the quadratic sound pressure on a considered point 1 is given by

$$p_1^2 = \sum_{j=1}^{N} p_{1,j}^2 \tag{A1}$$

where $p_{1,j}$ is the rms acoustic pressure due to the source j and N the number of discrete sources. In this case, the general expression of the NCSD between two points 1 and 2 is

$$\Phi_{1,2} = \frac{\sum_{j=1}^{N}\{p_{1,j}\,p_{2,j}\exp[-ik(d_{1,j} - d_{2,j})]\}}{\left[\sum_{j=1}^{N} p_{1,j}^2 \sum_{j=1}^{N} p_{2,j}^2\right]^{\frac{1}{2}}} \tag{A2}$$

where $d_{1,j}$ is the distance source j — point 1.

The modulus $||\Phi_{1,2}||$ of this complex number is representative of the coherence of the sound field (its maximum value 1 is found for a single source). The phase φ of the number allows the calculation of the sound propagation direction, knowing the sound speed and the distance between the considered points.

In the presence of a reflective ground, the sources of the jet and of a parallel image jet are taken into account. Here, the NCSD is

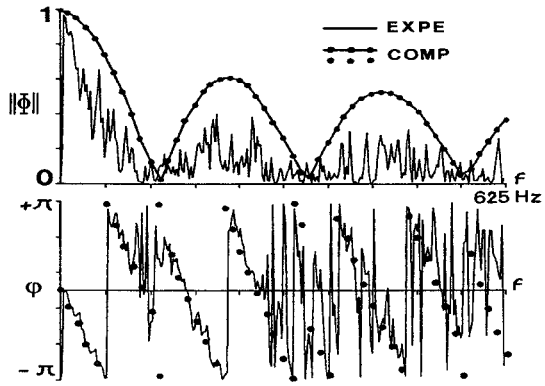

Fig. A1 Firing of rocket 0: experimental (EXPE) and computed (COMP) NCSD for two microphones close to the nozzle exit plane: $\|\Phi\|$ = modulus or coherence and φ = phase.

computed between two microphones near the nozzle exit plane (see Fig. 6). Figure A1 represents real and computed NCSD relative to the firing of rocket 1. The good agreement between computation and measurement shows that the spatial characteristics of direct and reflected sound fields are correctly simulated (see the phase unevenness). However, the recorded coherence is not as good as the calculated one, perhaps because the real sources are not concentrated on the jet axis. The random character of the noise and the rear echo due to the wall may also disrupt the signal.

Appendix B: Directivity

Figure 5 shows the directivity curves $f(\theta)$ given in Ref. 19. Here, the nozzle is considered as the origin of the sound field, which constitutes a far-field approximation. We have assumed that this directivity was suitable at a distance R from the nozzle equal to $10L_P$. In Fig. B1, S is the sound power peak ($OS = L_P$).

However, a nozzle-centered directivity (source O, angles θ) does not appear to be adapted to simulate the sound field near the jet because of the spreading of the real sound sources downstream from the nozzle. A better approximation for the near field is to consider that the dominant source is the sound power peak and that its directivity is the mean directivity of the other sources located upstream and downstream on the jet axis.

Knowing the directivity index $M(\theta)$ of source O, the corresponding directivity index $M(\theta')$ of source S must be corrected by the quantity 10 log (R'^2/R^2): indeed, the sound power integrated on a sphere (Σ) centered on source O, or integrated on a sphere (Σ') of same radius centered on source S, may be unchanging.

Figure B2 shows the directivity curves $f(\theta)$ and $f(\theta')$ for a given Strouhal number. We can see that the peak of the modified curve $f(\theta')$ is shifted of about 5 deg in the upstream direction. The changes of the directivity indices remain in the range [−2 dB; +2 dB], but are sufficient to improve in a appreciable manner the near-field simulation.

Appendix C: Theoretical Diameter of the Fully Expanded Jet

Knowing the chamber conditions P_i, T_i, γ_i, and r, the mass flow m_t, and the nozzle shape, the exhaust and fully expanded jet parameters can be calculated from ideal gas fluid dynamics equations. Thus, the theoretical diameter of the fully expanded jet (where pressure is equal to the ambient pressure P_a) may be deduced from the approximation $P_x \cdot S_x \approx$ const:

$$D_j \approx D_e[P_e/P_a]^{\frac{1}{2}} \tag{C1}$$

Tam and Tanna[21] propose a more precise formula related to the Mach numbers:

$$D_j = \left[\frac{1+0.5(\gamma-1)M_j^2}{1+0.5(\gamma-1)M_e^2}\right]^{[(\gamma+1)/4(\gamma+1)]} \left[\frac{M_e}{M_j}\right]^{\frac{1}{2}} D_e \tag{C2}$$

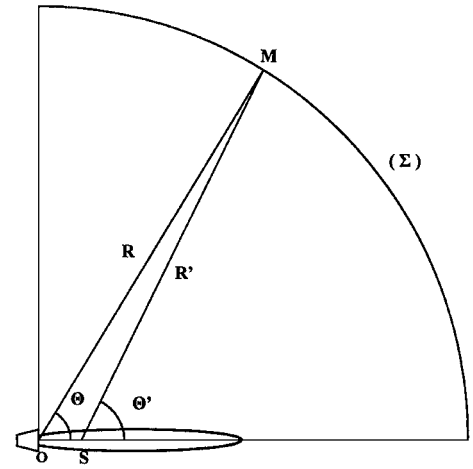

Fig. B1 Geometrical references for the calculation of the near-field directivity, referred to source S and angle θ', knowing the far-field directivity, referred to source O and angle θ.

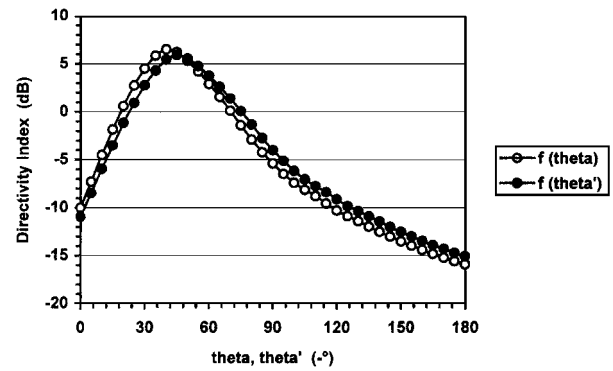

Fig. B2 Comparison between far-field directivity $f(\theta)$ and near-field directivity $f(\theta')$, for a dimensionless frequency equal to 0.0125.

where the ratio of the specific heats γ is assumed constant. In both formulas (C1) and (C2), the jet exhaust diameter D_e is assumed equal to the nozzle exit diameter.

In fact, the estimation of the jet exhaust parameters D_e, P_e, and M_e is not necessary. Consider the ideal gas state equation for a location x in the jet and the assumed mass flow conservation:

$$P_x = \rho_x r T_x \tag{C3}$$

$$m_t = \rho_x S_x V_x \tag{C4}$$

By substitution of ρ_x, we obtain an exact expression of $P_x\ S_x$:

$$P_x S_x = r m_t T_x / V_x \tag{C5}$$

Knowing that $S_x = \pi D_x^2/4$ and $c_x^2 = \gamma_x r T_x$, we can write, for the fully expanded jet,

$$P_a \pi D_j^2 \big/ 4 = m_t c_j^2 \big/ \gamma_j V_j \tag{C6}$$

After introduction of the Mach number $M_j = V_j/c_j$, the square root gives Eq. (13):

$$D_j = (2/M_j)(m_t V_j/\pi P_a \gamma_j)^{\frac{1}{2}} \tag{C7}$$

For jet IV of Table 3 ($\gamma = 1.355$), Eqs. (C1), (C2), and (C7) give, respectively, $D_j = 4.2$, 4.8, and 4.9 cm. For rocket F($\gamma = 1.22$), we obtain $D_j = 11.6$, 10.2, and 10.2 cm. More generally, Eqs. (C2) and (C7) appear to be in very good agreement.

Acknowledgments

This work was supported by the Centre National d'Etudes Spatiales (Direction des Lanceurs, Evry) and ONERA (Département de Simulation Numérique et Acoustique, Châtillon).

References

[1]McInerny, S. A., "Rocket Noise-A Review," AIAA Paper 90-3981, Oct. 1990.

[2]Pietrasanta, A. C., "Noise Measurements Around Some Jet Aircraft," *Journal of the Acoustical Society of America*, Vol. 28, No. 3, 1956, pp. 434–442.

[3]Morgan, W. V., and Young, K. J., "Studies of Rocket Noise Simulation with Substitute Gas Jets and the Effect of Vehicle Motion on Jet Noise," Rept. ASD-TDR 62-787, Wright–Patterson AFB, OH, March 1963.

[4]Morgan, W. V., Sutherland, L. C., Young, K. J., et al., "The Use of Acoustic Scale-Models for Investigating Near Field Noise of Jet and Rocket Engines," U.S. Air Force Wright Research and Development Center, Rept. WADD TR 61-178, Wright–Patterson AFB, OH, April 1961.

[5]Mayes, W. H., Landford, W. E., and Hubbard, H. H., "Near-Field and Far-Field Noise Surveys of Solid-Fuel Rocket Engines for a Range of Nozzle Exit Pressures," NASA TN D-21, Aug. 1959.

[6]Cole, J. N., Von Gierke, H. E., Kyrasis, D. T., Eldred, K. M., and Humphrey, A. J., "Noise Radiation from Fourteen Types of Rocket in the 1000 to 130,000 Pound Thrust Range," U.S. Air Force Wright Research and Development Center, TR 57-354, Wright–Patterson AFB, OH, Dec. 1957.

[7]Cole, J. N., England, R. T., and Powell, R. G., "Effects of Various Exhaust Blast Deflectors on the Acoustic Noise Characteristics of 1,000 Pound Thrust Rockets," U.S. Air Force Wright Research and Development Center, WADC TR 60-6, Wright–Patterson AFB, OH, Sept. 1960.

[8]Tedrick, R. N., "Acoustical Measurements of Static Tests of Clustered and Single-Nozzled Rocket Engines," *Journal of the Acoustical Society of America*, Vol. 36, No. 11, 1964, pp. 2027–2032.

[9]Wilhold, G. A., Guest, S. H., and Jones, J. H., "A Technique for Predicting Far Field Acoustic Environments Due to a Moving Rocket Sound Source," NASA TN D-1832, Aug. 1963.

[10]Lighthill, M. J., "On Sound Generated Aerodynamically, Part I, General Theory," *Proceedings of the Royal Society of London*, Vol. 211, No. A-1107, 1952, pp. 564–587.

[11]Lighthill, M. J., "On Sound Generated Aerodynamically, Part II, Turbulence as a Source of Sound," *Proceedings of the Royal Society of London*, Vol. 222, No. A-1148, 1954, pp. 1–32.

[12]Potter, R. C., and Crocker, M. J., "Acoustic Prediction Methods for Rocket Engines, Including the Effects of Clustered Engines and Deflected Exhaust Flow," NASA CR-566, Oct. 1966.

[13]Nagamatsu, H. T., and Horvay, G., "Supersonic Jet Noise," AIAA Paper 70-237, Jan. 1970.

[14]Stone, J. R., "Interim Prediction Method for Jet Noise," NASA TM X-71618, Nov. 1974.

[15]Seiner, J. M., "Advances in High Speed Jet Aeroacoustics," AIAA Paper 84-2275, Oct. 1984.

[16]Potter, R. C., "An Investigation to Locate the Acoustic Sources in a High Speed Jet Exhaust Stream," Wyle Labs., Rept. WR 68-4, NASA CR-101105, Feb. 1968.

[17]Ffowcs Williams, J. E., "The Noise from Turbulence Convected at High Speed," *Philosophical Transactions of the Royal Society of London*, Vol. 255, No. A-1061, 1963, pp. 469–503.

[18]Guest, S. H., "Acoustic Efficiency Trends for High Thrust Boosters," NASA TN D-1999, July 1964.

[19]Eldred, K. M. et al., "Acoustic Loads Generated by the Propulsion System," NASA SP-8072, June 1971.

[20]Candel, S., "Analysis of the Sound Field Radiated by the Ariane Launch Vehicle During Lift-off," *La Recherche Aérospatiale*, No. 1983-6, 1984, pp. 17–33.

[21]Sutherland, L. C., "Progress and Problems in Rocket Noise Prediction for Ground Facilities," AIAA Paper 93-4383, Oct. 1993.

[22]Tam, C. K. W., and Tanna, H. K., "Shock Associated Noise of Supersonic Jet from Convergent–Divergent Nozzle," *Journal of Sound and Vibration*, Vol. 81, No. 3, 1982, pp. 337–358.

[23]Norum, T. D., "Screech Suppression in Supersonic Jets," AIAA Paper 82-0050, Jan. 1982.

[24]Michalke, A., and Michel, U., "Prediction of Jet Noise in Flight from Static Tests," *Journal of Sound and Vibration*, Vol. 67, No. 3, 1979, pp. 341–367.

[25]Mc Inerny, S. A., Wichiser, J. K., and Mellen, R. H., "Rocket Noise Propagation," Symposium on Radiation and Scattering of Sound, IMECE, Nov. 1997.

[26]Mc Inerny, S. A., "The Broadband Noise Generated by Very High Temperature, High Velocity Rocket Exhausts," 2nd International Congress on Recent Developments in Air and Structure Borne Sound and Vibration, March 1992.

[27]Anderson, A. R., and Johns, F. R., "Characteristics of Free Supersonic Jets Exhausting into Quiescent Air," *Jet Propulsion*, Jan. 1955, pp. 13–15, 25.

[28]Gély, D., Varnier, J., Piet, J. F., and Prévost, M., "Experimental Study of Scale Effect on the Noise Generated by Solid Rockets," 3e Congrès Français d'Acoustique, May 1994.

[29]Piet, J. F., and Elias, G., "Airframe Experimental Techniques for Source Location," AIAA Paper 97-1643, May 1997.

[30]Mosher, M., "Phased Arrays for Aeroacoustic Testing: Theoretical Development," AIAA Paper 96-1713, May 1996.

P. J. Morris
Associate Editor